Japanese Journal of Applied Physics
Vol. 45, No. 3B, 2006, pp. 1956–1961

Electronic Structures of Individual Poly(3-hexylthiophene) Nanowires on Hydrogen-Terminated Si(100) Surfaces

Yasuhiko TERADA*, Hidemi SHIGEKAWA, Yuji SUWA[1], Seiji HEIKE[1], Masaaki FUJIMORI[1] and Tomihiro HASHIZUME[1]

Institute of Applied Physics, CREST, 21st COE, University of Tsukuba, Tsukuba, Ibaraki 305-8573, Japan
[1]*Advanced Research Laboratory, Hitachi, Ltd., Hatoyama, Saitama 350-0395, Japan*

(Received July 5, 2005; accepted September 4, 2005; published online March 27, 2006)

Electronic structures of individual conducting polymers, poly(3-hexylthiophene)s (P3HTs), fixed on a hydrogen-terminated Si(100) surface have been examined by scanning tunneling microscopy/spectroscopy and first-principles calculations within the density-functional approach. The calculations reveal that the electronic structure of the polymer is only weakly influenced by the substrate, which ensures that the fixed polymers maintain a conduction property similar to that of isolated polymers. The current–voltage curves for the substrate-molecule-tip junction show rectification characteristics, indicating the carrier doping in the fixed polymers. [DOI: 10.1143/JJAP.45.1956]

KEYWORDS: scanning tunneling microscopy/spectroscopy (STM/STS), first-principles calculation, electronic structures, conducting polymer, P3HT, Si(100)

1. Introduction

Electronics using organic molecules may have a great advantage in mass-producing homogenous and flexible devices at low cost by chemical synthesis, over traditional semiconductor electronics.[1)] Although much progress has been made in synthesizing individual molecular components, there still remain immense and unsolved difficulties in economical fabrication of complete electronic circuits at the molecular level. A possible solution is hybrid molecular electronic devices,[1)] comprising molecular components and wires that connect to metal electrodes fabricated on a semiconductor substrate. In such hybrid devices, organic molecules are desirable for intermediate wires connecting molecular components and metal electrodes because they would exhibit similar electronic structures and hence can be utilized to tune their interfacial energy barriers.[2)]

Contact between molecular wires (or components) and substrates, however, could be a serious problem that can limit the performance and stability of the devices. The presence of the substrate surface may have an influence on electronic structures of the embedded molecules as a result of bond formation and may alter the designed performance of molecular wires. Therefore, understanding of the contact effect on the electronic structures is a key issue to designing hybrid devices.

Poly(3-hexylthiophene)s (P3HTs) fixed on a hydrogen-terminated Si(100) surface [H-Si(100)] could be a model system to investigate energy structures of molecular wires embedded on substrate surfaces because it is likely that the hydrogen passivation of the surface enables the preservation of the energy structures of the P3HT wires. Moreover, it has been suggested that the embedded P3HTs can be utilized for molecular wires, together with fabrication techniques that enable the patterning of microscopic electrodes in the planar configuration on H-Si(100) surfaces.[3–5)] We have investigated the electronic structures of individual P3HTs fixed on H-Si(100) using scanning tunneling microscopy and spectroscopy (STM/STS).[6)] The energy-band diagram and conduction model have been proposed for the H-Si(100)/P3HT/STM-tip system. The assumptions in the previous paper[6)] are (i) no band bending of bulk silicon, (ii) a band picture for the electronic structure of P3HT, (iii) a weak interaction between P3HT and H-Si(100), and (iv) bias-dependent molecular orbital (MO) levels. Although the previous model has given an explanation consistent with the experimental results, some of the assumptions were difficult to be proved by the experiments alone. To give a complementary explanation, we calculate here the electronic structures of the P3HT/H-Si(100) system within the density-functional approach. We reexamine the previous model in accordance with the calculations and confirm the validity of the model. We then explain the experimental results consistently.

2. Experimental

Silicon samples were cut from a commercial n-type Si(100) wafer (1–6 mΩ·cm) doped with arsenic. Methods for preparing the H-terminated surface and W tips are described elsewhere.[4)] P3HTs were dissolved in chloroform solvent and the solution was pulse injected onto H-Si(100) using a pulse valve (General Valve) as previously reported.[7,8)] After removing the residual solvent by annealing the silicon substrate, we obtained STM images and confirmed that isolated chains of P3HT were successfully mounted on the clean H-Si(100) surface.

All the STM/STS measurements were carried out at room temperature under a base pressure of the STM chamber of 1×10^{-8} Pa. During STS measurements, the STM tip position was held constant at the height established by the constant current feedback conditions of V_s and I, and then the I–V curve was acquired within the disabled feedback loop. At each position, the corresponding I–V curve was averaged over 32 scans to increase the signal-to-noise ratio. A simultaneously acquired topographic image ensured an accurate assessment of the spatial position of each spectrum. The typical numbers of topographic and spectroscopic data points were 256×256 and 64×64, respectively. The conductance spectra, dI/dVs, were numerically differentiated from the measured I–Vs.

The calculations were based on the density functional

*Author to whom correspondence should be addressed.
E-mail address: terada@bk.tsukuba.ac.jp

theory. We have employed the generalized gradient approximation (GGA)[9] and used the plane-wave-based ultrasoft pseudopotentials.[10,11] The energy cutoff was taken as 20.25 Ry. The convergence criterion of the geometry optimization was that all of the forces acting on each atom were within 1×10^{-3} hartree/a.u. The polymers were assumed to exhibit an infinite periodic structure with a unit cell including two pentagons. The H-Si(100) surface was represented by a slab model containing five layers of Si atoms. The remaining dangling bonds of an unreconstructed Si surface on the back of the slab were terminated with H atoms.

3. Results

3.1 STM image and STS spectra

Figure 1(a) shows a typical topographic image of a P3HT/H-Si(100) surface. Isolated chains of P3HT are observed in this figure, and the width, length, and height are in good agreement with the typical values in our previous STM observations.[7,8] The current maps at different substrate voltages are shown in Figs. 1(b)–1(d). There is a distinct difference in the maps between the positive and negative bias voltages. The maps at negative bias [Figs. 1(c) and 1(d)] exhibit little contrast, whereas that at positive bias [Fig. 1(b)] exhibits a distinct contrast, reflecting the difference in the I–V curves between P3HT and H-Si(100). The dark and bright areas in Fig. 1(b) are assigned to the P3HT and H-Si(100) surface sites, respectively.

To quantitatively discuss the I–V difference, the I–V data were averaged over the dark (P3HT) and bright [H-Si(100)] areas in Fig. 1(b). Figures 1(e) and 1(f) show the resulting I–V curves and dI/dV spectra for P3HT (open circles) and H-Si(100) (solid circles). The I–V and dI/dV curves for H-Si(100) form symmetric shapes about a symmetry axis of $V_s = -0.40$ V and exhibit a conductance gap at $-0.94 < V_s < 0.13$ V.

In contrast to those for the H-Si(100) surface, the I–V curve and dI/dV spectrum for P3HT [Figs. 1(e) and 1(f)] are highly asymmetric and have two features: (i) a conductance gap at $-0.94 < V_s < 0.73$ V that stretches out toward the positive bias axis, in contrast to that of H-Si(100), and (ii) current suppression at positive bias, revealing a rectification characteristic.

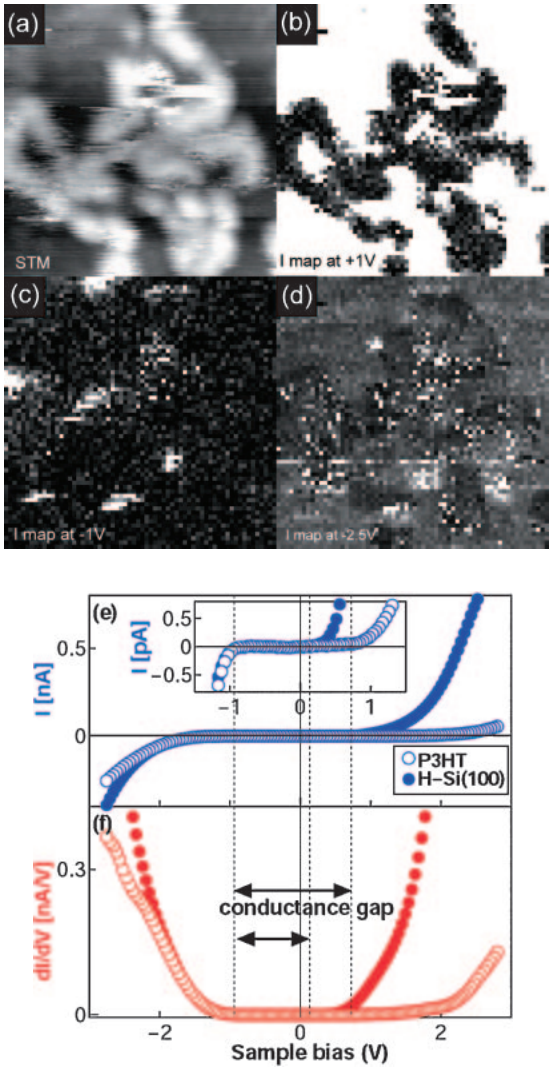

Fig. 1. (a) STM topographic image of P3HT/H-Si(100) ($20 \times 20\,\mathrm{nm}^2$, $V_s = -2$ V, $I = 0.05$ nA). (b)–(d) Spatial maps of I obtained by recording I–V curves simultaneously with topographic image shown in (a). The maps were taken at (b) $V_s = +1$ V, (c) $V_s = -1$ V, and (d) $V_s = -2.5$ V. (e) Spatially averaged I–V curves for P3HT (open circle) and H-Si(100) (solid circle). (f) dI/dV curves numerically differentiated from the I–V curves shown in (e) for P3HT (open circle) and H-Si(100) (solid circle).

3.2 Calculations

The calculations for the P3HT/H-Si(100) system are time consuming because of a large unit cell. We first examine the possibility that P3HT can be substituted for polythiophene (PT) that has a less-complicated chemical structure. It is likely that the similarity in chemical structure between PT and P3HT results in electronic structures similar to each other. As expected, the calculated bands and density of states (DOS) of PT [Figs. 2(a) and 2(b)] and P3HT [Figs. 3(a) and 3(b)] are quite similar, especially near the Fermi levels. For both PT and P3HT, the amplitudes of wave functions near the Fermi levels [Figs. 2(d)–2(g) and 3(d)–3(g)] are located at the pentagon sites, indicating their conducting (or semiconducting) properties along the backbones. Their band features only differ at the levels much lower than the Fermi level [Figs. 2(h) and 3(h)]. The low-energy bands for P3HT [Fig. 3(h)] are attributed to a side chain of the hexyl group. Although the side chain affects the structural properties such as the twisting of the molecular backbone [see inset of Fig. 3(c)], the conduction property is mainly related to the bands near the Fermi energy. Thus, we hereafter substitute polythiophene (PT) for P3HT in the calculations.

We then calculate the band structures and DOS for H-Si(100) [Fig. 4(c)] and the PT/H-Si(100) system [Fig. 4(d)] along with the geometry optimization [Figs. 4(a) and 4(b)]. A 4×4 unit cell of silicon coincidentally has a similar length with the size of four pentagons of PT in the optimized structure, and hence it is found that only a vertical extension of a unit cell is sufficient for calculations. Figure 4(d) reveals that the valence band (VB) of PT (drawn by a dashed line), located in the band gap of H-Si(100), forms a shape similar to that of the isolated PT-VB and is not affected by the presence of H-Si(100). This indicates the absence of strong bonds between PT and H-Si(100). This is also confirmed by the calculations of the wave functions (Fig. 5). The amplitudes of the highest occupied molecular orbital

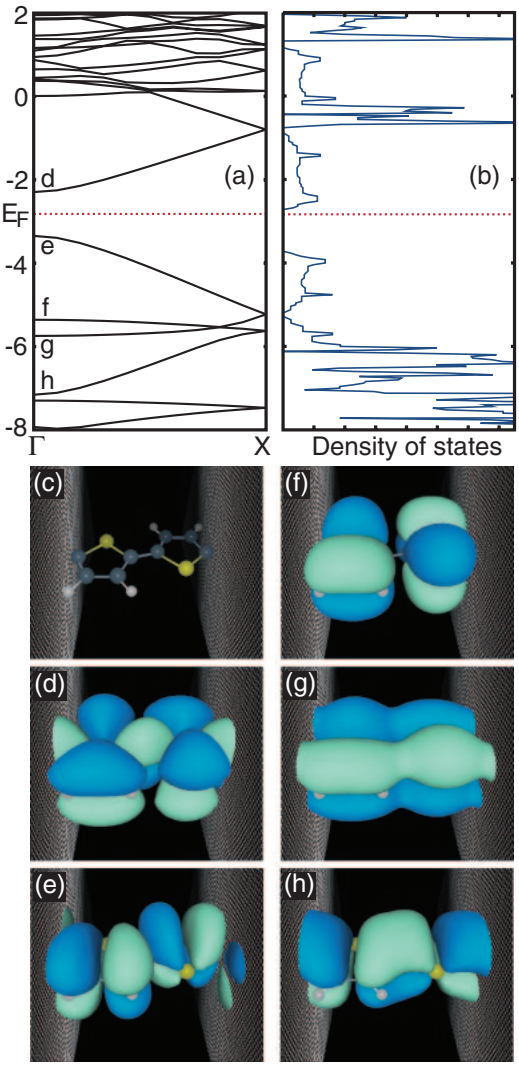

Fig. 2. Calculations of energy structures of PT. (a) Band structures. (b) DOS. (c) Optimized geometry. (d)–(h) Amplitudes of wave functions at Γ-point in (d) LUMO, (e) HOMO, (f) HOMO-1, (g) HOMO-2, and (h) HOMO-3 states. The corresponding band structures are shown in (a).

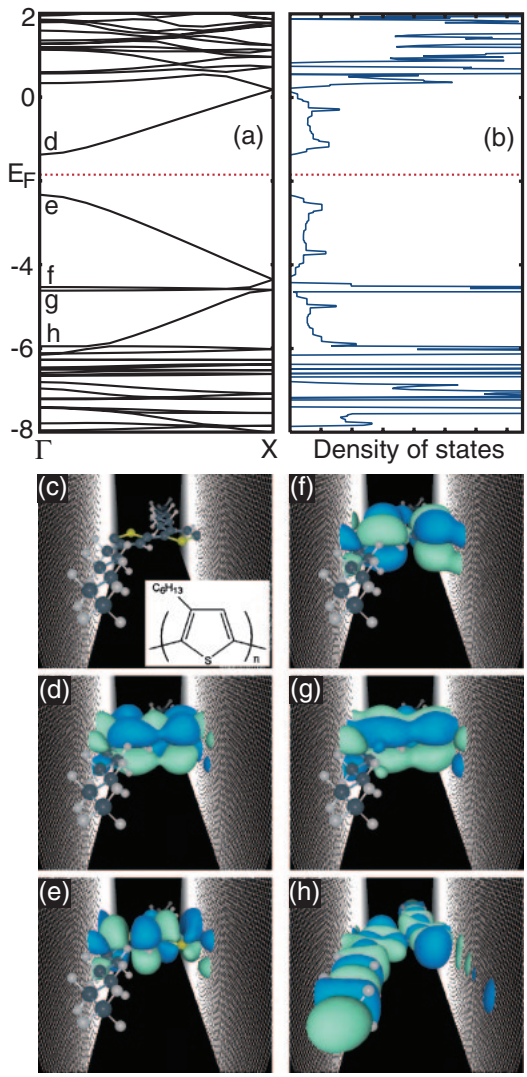

Fig. 3. Calculations of energy structures of P3HT. (a) Band structures. (b) DOS. (c) Optimized geometry. (d)–(h) Amplitudes of wave functions at Γ-point in (d) LUMO, (e) HOMO, (f) HOMO-1, (g) HOMO-2, and (h) HOMO-3 states. The corresponding band structures are shown in (a). The chemical structure of P3HT is shown in the inset of (c).

(HOMO), HOMO-1, and HOMO-2 states [Figs. 5(b)–5(d)] are located at either the PT or H-Si(100) site, except for the LUMO state exhibiting a slightly overlapping amplitude [Fig. 5(a)].

4. Discussion

4.1 Model

On the basis of the calculations, we examine the model that was previously proposed.[6] We have assumed (i) the absence of the band bending in the bulk silicon, (ii) the band picture for the electronic structure of P3HT, (iii) a weak interaction between P3HT and H-Si(100), and (iv) bias-dependent molecular energy-band levels. Here, we ignore the band-bending effect as previously discussed because the silicon we used is so highly doped ($2 \times 10^{19}\,\mathrm{cm}^{-3}$) that the depletion layer is sufficiently thin (1 nm) to enable electrons to tunnel through it.[12] The band picture for P3HT energy levels is a consequence of the calculations under the periodical boundary condition, as revealed by the continuous PT-DOS on H-Si(100) [Fig. 4(d)]. The weak interaction between P3HT and H-Si(100) is confirmed by the calculations as discussed before. The absence of the strong bonds between the molecule and the substrate surface results in the bias-dependent molecular bands,[12–14] because the electric field inside the molecule is poorly screened and hence shifts the molecular electrostatic potential.

Under these assumptions, we have modeled the energy-band diagram for the H-Si(100)/P3HT/W-tip junction (Fig. 6) as previously proposed.[6] Although silicon band bending is shown in this figure, we assume $\phi_{Si} = 0$ as in case of the H-Si(100)/W-tip system. Taking the molecular band shift into account, the shift of the electrostatic potential on P3HT is roughly given by $\eta(V_S - \phi_{Si}) \approx \eta V_S$ under a bias V_S, where η denotes the average molecular potential under unit applied bias.[12] The parameter η is determined by the geometry of the junction; it is approximately 0.5 when an STM tip touches the molecule and decreases with increasing tip–molecule distance.[9] The energy gap of P3HT is assumed to be a typical experimental value in the literature, 2.1 eV.[15] We adjust the location of the molecular bands under zero bias in such a way that P3HT-VBM is located in the silicon

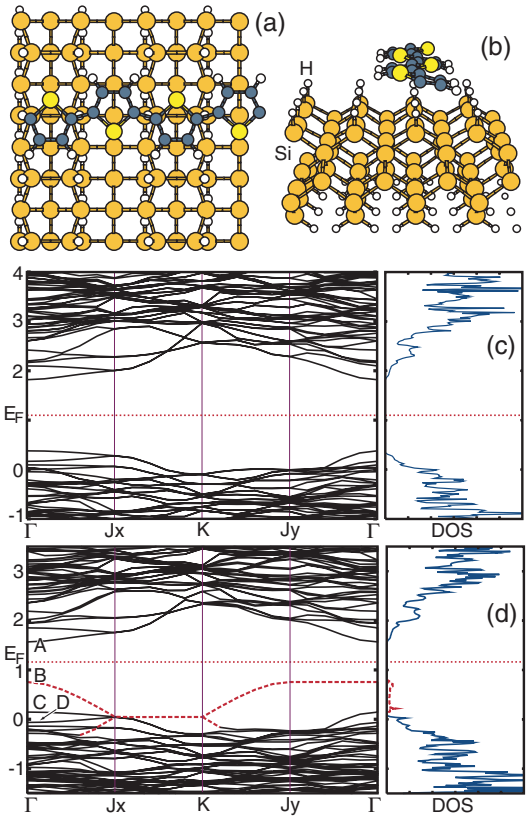

Fig. 4. Calculations of energy structures of H-Si(100) and PT on H-Si(100). [(a) and (b)] Optimized geometry of PT on H-Si(100) in (a) top view and (b) side view. (c) Band structure and DOS of H-Si(100). (d) Band structure and DOS of PT on H-Si(100). The dashed line corresponds to states attributed to PT.

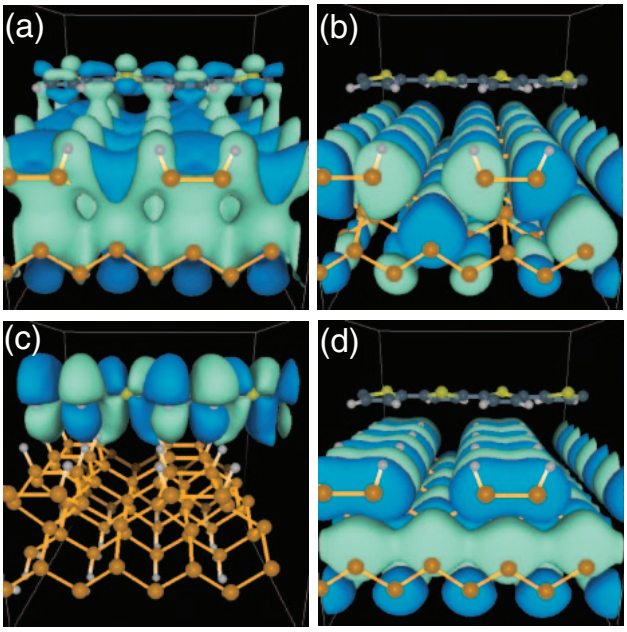

Fig. 5. Amplitudes of wave functions calculated for PT on H-Si(100) at Γ-point in (a) LUMO, (b) HOMO, (c) HOMO-1, and (d) HOMO-2 states, respectively.

band gap as revealed by the calculations [Fig. 4(d)]. The location agrees well with the expectations in our previous paper.[6)]

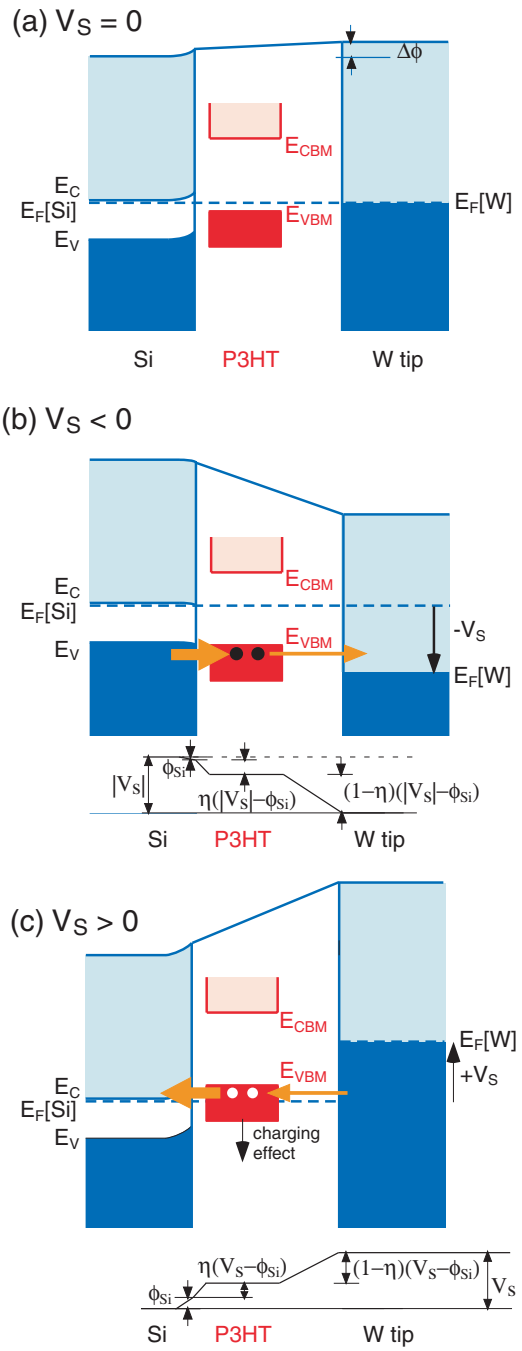

Fig. 6. Energy band diagrams in H-Si(100)/P3HT/STM tip junction. E_C, E_V, E_{CBM}, and E_{VBM} are energy levels of silicon-CBM, silicon-VBM, P3HT-CBM, and P3HT-VBM, and E_F[Si] and E_F[W] are Fermi energy levels of silicon and the W tip, respectively. ϕ_{Si} and $\Delta\phi$ are silicon band bending and the work-function difference between silicon and tungsten, respectively. Electrostatic potential profiles are also shown at the bottom in (b) and (c).

As a result of the molecular band shift, the conductance gap in the molecular I–V is determined by the shift of either CBM or VBM of P3HT, and the closer band edge to either CBM or VBM of silicon determines the conduction behavior. In our case, therefore, P3HT-VBM is expected to dominate the conduction. This is also in good agreement with the previous conclusion that the conductance gap is determined by the shift of P3HT-VBM.[6)]

4.2 Conduction gaps in I–V curves

In accordance with the model, we explain the experimental results as follows. We first consider the *I–V* curve at the H-Si(100) sites [Figs. 1(e) and 1(f)]. Ignoring the band-bending effect, the measured conductance gap (1.07 V) for H-Si(100) is attributed to the band gap of bulk silicon. The gap is shifted toward the negative V_s axis because the Fermi energy E_F[Si] of bulk silicon is close to the energy level of bulk-silicon-CBM.

We then consider the *I–V* curve at the P3HT sites. The measured *I–V* curve shows the wide conductance gap and the rectification. The conductance gap can be explained by the P3HT-VB-based conduction model. Under a slight positive or negative bias, the band gap of P3HT prevents electrons from tunneling through the junction. Under a large negative bias, the tip Fermi energy E_F[W] becomes lower than the silicon-VBM level, E_V [Fig. 6(b)]. Since the P3HT-VB levels exist in between them, electrons in the P3HT-VB tunnel into the tip empty states while the P3HT-VB levels are filled by the silicon-molecule coupling, which is stronger than the molecule-tip coupling. Under a large positive bias, on the other hand, the P3HT-VBM level, E_{VBM}, becomes higher than the silicon-CBM level, E_C [Fig. 6(c)]. In this case, the P3HT-VB levels are emptied out and holes are formed in P3HT-VB, leading to the electron tunneling from the tip filled states. According to our previous investigation,[6] the threshold for tunneling is given by the conditions $E_V > E_F$[W] for $V_s < 0$ and $E_C < E_{VBM}$ for $V_s > 0$.

4.3 Origins of rectification

We then explain the suppression of the current at positive bias. In our previous paper,[6] we discussed three possible reasons for the current suppression: (i) the different coupling of the P3HT-MOs to the silicon orbitals, (ii) the silicon band bending, and (iii) the charging effect of P3HT. Among them, we have concluded that the former two are unlikely and the charging effect is likely. In addition to the charging effect, there is one other important reason that has not been discussed previously. The forth and prominent reason for the suppression is the difference in the number of states of P3HT that contribute to current flow between negative and positive biases. The electrons tunnel via the P3HT-VB levels that have higher energies than E_F[W] at negative bias, while via the P3HT-VB levels that have higher energies than E_C at positive bias. Therefore, the number of states that contribute to tunneling is larger at negative bias than at positive bias. In the Tersoff–Hamann approximation,[16] tunneling conductance can be generally expressed by $dI/dV \propto \rho_S(eV - E_F)$, where ρ_S and E_F are the DOS and Fermi energy of a surface. Using this approximation, the molecular conductance is roughly given by $dI/dV \propto (1-\eta)\rho_{P3HT}((1-\eta)eV_S)$ for $V_S(\leq V_a) < 0$ and $dI/dV \propto \eta\rho_{P3HT}(\eta eV_S)$ for $V_S(\geq V_b) > 0$, where ρ_{P3HT} is the DOS of P3HT, and V_a (< 0) and V_b (> 0) are the threshold voltages for tunneling. Since we assume $0 < \eta \leq 0.5$, we can derive the relationship that the conductance dI/dV is larger for $V_S < 0$ than for $V_S > 0$, provided that ρ_{P3HT} is constant. Considering the simplicity of our theoretical approach, this accounts well for the current suppression at positive bias.

The charging effect is weak compared with the DOS effect but not negligible. The effect of differential charging on the *I–V* asymmetry has previously been discussed in detail[17] for a system where two contacts are asymmetric. When this is the case, one contact is much stronger than the other. At negative bias, the stronger silicon–P3HT contact tends to fill the P3HT-VB levels, leading to no energy shift of P3HT-MO levels due to the charging. At positive bias, however, the P3HT-VB levels tend to be emptied out by the stronger silicon–P3HT contact, leading to the positive charging of P3HT, which shifts all the energy levels down. This shift, not present for negative bias, would postpone the onset of conduction and effectively stretch out the voltage axis toward the positive bias region.

The above argument indicates that the P3HT molecule is positively doped at positive substrate bias. We therefore conjecture that the STM tip serves as a gate electrode to enable the p-type P3HT doping. Applying the negative bias to the tip would cause the modulation of the conduction behavior through the P3HT backbone.

5. Conclusions

In summary, we investigated the electronic structures of the H-Si(100)/P3HT/STM-tip system experimentally and theoretically. The measured *I–V* curves reveal (i) the shift of the onset voltage toward the positive substrate bias axis, in contrast to the curves for the H-Si(100)/tip system, and (ii) the suppression of the current at positive substrate bias. The first-principle calculations reveal that the molecular energy bands are little affected by the presence of H-Si(100) and the molecular VB is located in the silicon band gap. In accordance with the calculations, we examined the model for the electrostatic potential profile across the H-Si(100)/P3HT/W-tip junction that was previously proposed, and confirmed the validity of the model. The measured *I–V* asymmetry is explained by the shift of the P3HT-VB levels driven by the STM tip potential. The suppression of the current arises from the difference in the number of states of P3HT that contribute to current flow between negative and positive biases. The tunneling at positive bias causes the charging of P3HT, indicating the possibility of electrical doping of the polymer wire by applying a negative voltage to the STM tip.

Acknowledgement

Part of the study was performed through Special Coordination Funds for Promoting Science and Technology of the Ministry of Education, Culture, Sports, Science and Technology of Japan.

1) C. Joachim, J. K. Gimzewski and A. Aviram: Nature (London) **408** (2000) 541.
2) I. H. Campbell, S. Rubin, T. A. Zawodzinski, J. D. Kress, R. L. Martin, D. L. Smith, N. N. Barashkov and J. P. Ferraris: Phys. Rev. B **54** (1996) R14321.
3) J. W. Lyding, T.-C. Shen, J. S. Hubacek, J. R. Tucker and G. C. Abeln: Appl. Phys. Lett. **64** (1994) 2010.
4) T. Hashizume, S. Heike, M. I. Lutwyche, S. Watanabe, K. Nakajima, T. Nishi and Y. Wada: Jpn. J. Appl. Phys. **35** (1996) L1085.
5) M. Fujimori, S. Heike, Y. Terada and T. Hashizume: Nanotechnology **15** (2004) S333.
6) Y. Terada, K. Miki, M. Fujimori, S. Heike, Y. Suwa and T. Hashizume: J. Appl. Phys. **97** (2005) 124302.
7) Y. Terada, B.-K. Choi, S. Heike, M. Fujimori and T. Hashizume: Nano

Lett. **3** (2003) 527.
8) Y. Terada, B.-K. Choi, S. Heike, M. Fujimori and T. Hashizume: J. Appl. Phys. **93** (2003) 10014.
9) J. P. Perdew, K. Burke and Y. Wang: Phys. Rev. B **54** (1996) 16533.
10) D. Vanderbilt: Phys. Rev. B **41** (1990) 7892.
11) K. Laasonen, A. Pasquarello, R. Car, C. Lee and D. Vanderbilt: Phys. Rev. B **47** (1993) 10142.
12) T. Rakshit, G.-C. Liang, A. W. Ghosh and S. Datta: Nano Lett. **4** (2004) 1803.
13) S. Datta, W. Tian, S. Hong, R. Reifenberger, J. I. Henderson and C. P. Kubiak: Phys. Rev. Lett. **79** (1997) 2530.
14) N. P. Guisinger, M. E. Greene, R. Basu, A. S. Baluch and M. C. Hersam: Nano Lett. **4** (2004) 55.
15) T.-C. Chung, J. H. Kaufman, A. J. Heeger and F. Wudl: Phys. Rev. B **30** (1984) 702.
16) J. Tersoff and D. R. Hamann: Phys. Rev. Lett. **50** (1983) 1998.
17) F. Zahid, A. W. Ghosh, M. Paulsson, E. Polizzi and S. Datta: Phys. Rev. B **70** (2004) 245317.